

Research



Cite this article: Harcourt WD, Briers RA, Huxham M. 2018 The thin(ning) green line? Investigating changes in Kenya's seagrass coverage. *Biol. Lett.* **14**: 20180227. <http://dx.doi.org/10.1098/rsbl.2018.0227>

Received: 29 March 2018

Accepted: 26 October 2018

Subject Areas:

environmental science, ecology

Keywords:

seagrass, mapping, Kenya, blue carbon

Author for correspondence:

William D. Harcourt

e-mail: wdharcourt1994@gmail.com

A contribution to the special feature 'Blue carbon' organized by Catherine Lovelock.

Global change biology

The thin(ning) green line? Investigating changes in Kenya's seagrass coverage

William D. Harcourt, Robert A. Briers and Mark Huxham

School of Applied Sciences, Edinburgh Napier University, Edinburgh, UK

WDH, 0000-0003-3897-3193; RAB, 0000-0003-0341-1203; MH, 0000-0001-7877-6675

Knowledge of seagrass distribution is limited to a few well-studied sites and poor where resources are scant (e.g. Africa), hence global estimates of seagrass carbon storage are inaccurate. Here, we analysed freely available Sentinel-2 and Landsat imagery to quantify contemporary coverage and change in seagrass between 1986 and 2016 on Kenya's coast. Using field surveys and independent estimates of historical seagrass, we estimate total cover of Kenya's seagrass to be 317.1 ± 27.2 km², following losses of 0.85% yr⁻¹ since 1986. Losses increased from 0.29% yr⁻¹ in 2000 to 1.59% yr⁻¹ in 2016, releasing up to 2.17 Tg carbon since 1986. Anecdotal evidence suggests fishing pressure is an important cause of loss and is likely to intensify in the near future. If these results are representative for Africa, global estimates of seagrass extent and loss need reconsidering.

1. Introduction

Despite the increasing sophistication of Blue Carbon science, some basic information remains imprecise. Prominent among this is the regional extent of seagrass habitats, which is essential in determining seagrass carbon (C) stocks and flows. Knowledge of seagrass coverage is globally variable; for example, the USA is well studied, representing 130 of the 215 sites detailed in a review of global trends [1]. By contrast, Africa remains poorly mapped, with paltry information on seagrass extent, ecology and C stocks [2]. Given the large areas and high C concentrations that may be present in Africa and other poorly researched tropical regions [3], current global estimates may be very inaccurate.

Blue Carbon habitats are globally threatened; indeed the estimated 7% yr⁻¹ loss of seagrass may be the worst trend for any global habitat [1]. Having good data on rates of decline and drivers of loss are essential. However, problems involved in mapping current seagrass coverage are magnified when estimating trends. Historical data are of widely varying accuracy with no information at all for many sites before the late 1970s and the first Landsat satellite images. The low radiometric resolution and spectral sensitivity of Landsat 1–5 imagery impedes seagrass mapping, particularly for sub-tidal areas. While the advent of high resolution, freely available imagery represents enormous progress, logistical and technical challenges remain in using these for seagrass monitoring and in deriving comparisons between current and historical data.

Here, we estimate current and historical seagrass coverage in Kenya. We produce the first national analysis of seagrass cover change that begins to address the large gap in knowledge from the African continent and allows comparison with better-known areas of the world. In addition, we aim to illustrate an approach of relevance to seagrass mapping in general. Our objectives were:

- 1) To map the contemporary coverage of seagrass on Kenya's coast using the highest resolution freely available imagery.

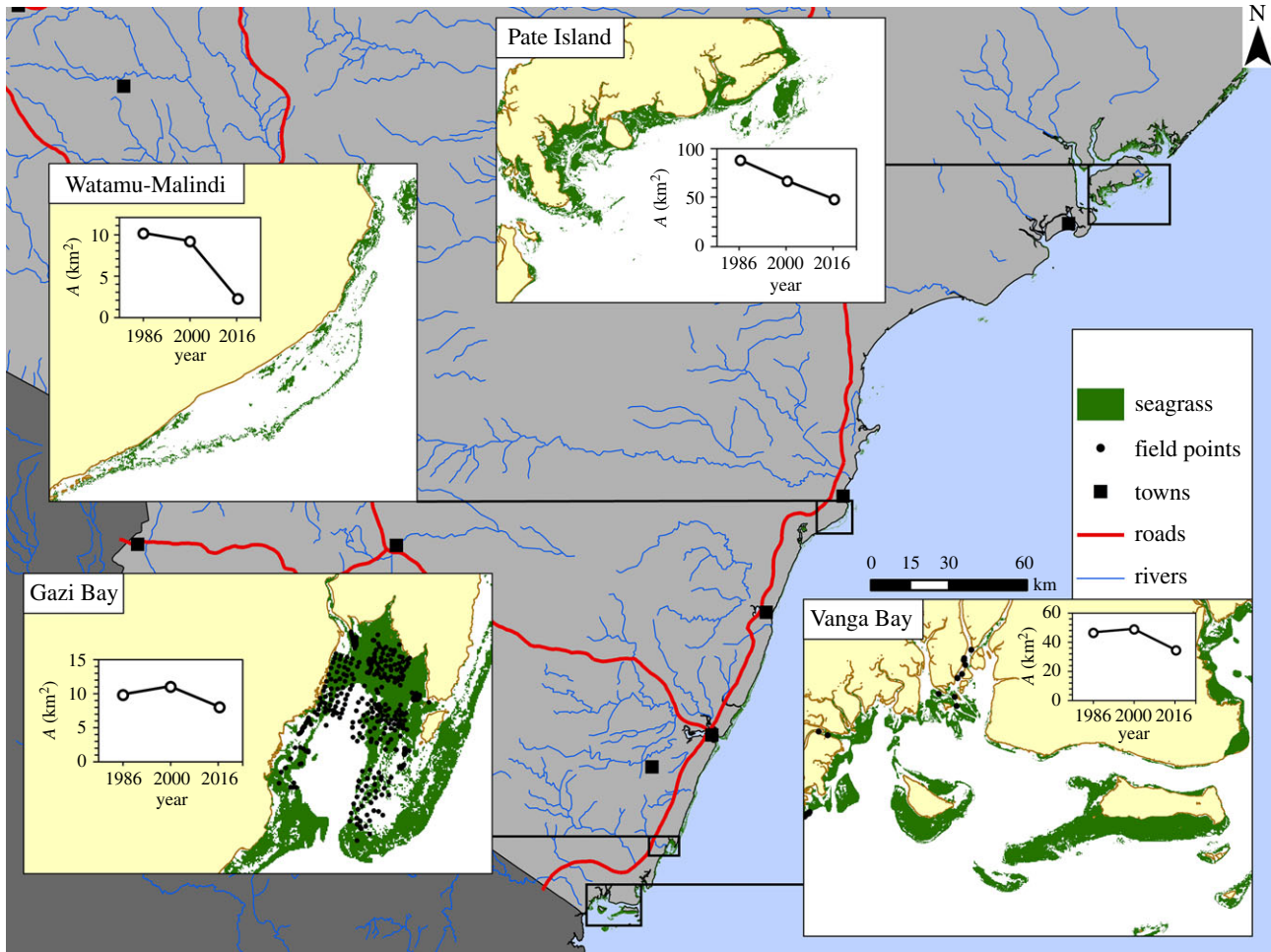


Figure 1. Seagrass coverage in Kenya. Inset panels display LC8 derived maps and temporal records for representative sites.

- 2) To reveal rates of change over the past 30 years and examine the implications for C storage and loss.

2. Methods

Seagrass coverage for 2016 was mapped using Landsat 8 (LC8) and Sentinel-2 (S2). Coverage in 2000 and 1986 were estimated using Landsat 7 (LE7) and Landsat 5 Thematic Mapper (LT5), respectively. Sen2Cor and LEDAPS were used to convert S2 and Landsat imagery, to Bottom-of-Amosphere reflectance and to remove clouds. Images were projected to WGS 1984 UTM zone 37 South coordinate system. Images were paired to represent high and low tide conditions. Water was separated from land by thresholding Normalized Difference Water Index values, and differenced between image pairs to extract image specific emergent and submerged zones. Correlating NIR reflectance with the visible wavelengths in deep water allowed us to correct for the specular reflection of light from the ocean surface [4].

The emergent region was classified using the ISODATA unsupervised classification method due to the absence of spatially distributed field data. Resultant classes were merged by assigning a similarity threshold to a dendrogram, computed from individual class attributes. Groups of pixels (approx. 10–20) were assessed, and the presence of seagrass determined by comparing reflectance profiles to ground-based spectral profiles [5], examining the original image, using local field knowledge, and reviewing all relevant literature and official reports on Kenyan seagrass.

For the submerged regions, we computed a relative water depth grid (WD_{rel}), based on the ratio between the linearized

blue (R_{Blue}) and green (R_{Green}) bands in each image [6], and isolated anomalies removed by using Segment Mean Shift within ArcGIS 10.5. The transition to deep water is signalled by a sudden drop in WD_{rel} , and a threshold used to exclude these pixels. Discrete zones of WD_{rel} were extracted using a quantile interval method, classified using the same approach as above, and corrected for the presence of coral by thresholding the ratio of the red to green band across all depths [7]. Such hierarchical classification schemes circumvent the effects of water depth changes to benthic reflectance [8].

Point measurements of seagrass presence and absence were recorded from Gazi Bay (432) and Vanga Bay (27) (figure 1) using a GoPro Hero 4 and a stratified random sampling technique in 2017 (see [9] for more information). Overall accuracy (OA) was derived from a confusion matrix between the field data and S2-derived seagrass coverage. The accuracy of LT5 (1986), LE7 (2000) and LC8 (2016) maps were determined by calculating two independent estimates for each time period, from separate image sets overlapping in time and space. A confusion matrix was derived from this overlap, and OA computed (Landsat image overlap method).

We mapped seagrass coverage for a single Landsat path and row scene across four dates between 2015 and 2016 to assess intra-annual and short-term variability and found it to be minimal [9].

We estimated total organic carbon (C_{org}) stored within Kenya's seagrass using the following equation:

$$\text{Total } C_{org} = A \times (\text{Biomass } C_{org} + \text{Sediment } C_{org}),$$

where A is total seagrass cover. Regional estimates of biomass C_{org} and sediment C_{org} for seagrasses in Gazi bay (figure 1) are

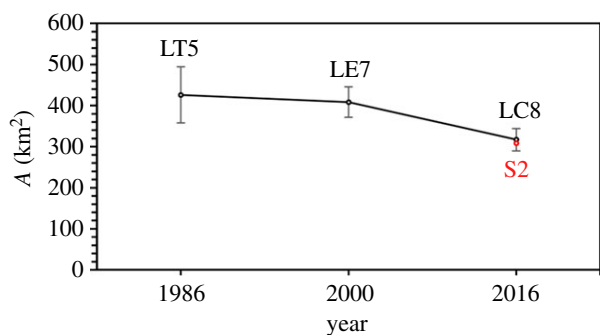


Figure 2. Changes in Kenyan seagrass coverage 1986–2016 using Landsat (black) and S2 (red). Error bars were calculated by multiplying the % residual accuracy by total coverage to give a \pm range.

$585 \pm 43 \text{ Mg C km}^{-2}$ and $23\,557 \pm 2\,437 \text{ Mg C km}^{-2}$ [3], respectively. In comparison, global seagrass biomass C_{org} and sediment C_{org} are estimated to be $251 \pm 48 \text{ Mg C km}^{-2}$ and $16\,560 \text{ Mg C km}^{-2}$, respectively [10]. Destruction of seagrass leads to loss of biomass C_{org} , whereas sediment C_{org} may stabilize or be rapidly lost [11]. Here we estimate maximum feasible C loss by assuming sediment C_{org} in the top 1 m reverts to $4967 \text{ Mg C km}^{-2}$ (the average value for unvegetated sediment reported in [3]) following seagrass loss.

3. Results

Seagrass extends along the coast of Kenya, with the exception of the Tana River delta, probably due to high turbidity (figure 1). Total 2016 seagrass coverage was estimated as $317.1 \pm 27.2 \text{ km}^2$ (LC8) and $308.4 \pm 40.8 \text{ km}^2$ (S2) (figure 2). Of this, 62% occurs north of Malindi (northern Kenya), particularly the Lamu Archipelago (figure 1). Southern Kenyan seagrasses occupy the reef crests, inlets and lagoons from Vanga Bay to Malindi (figure 1). Emergent seagrass (area exposed at the time of image acquisition) made up 64.2% of the total seagrass cover.

Kenya's seagrass declined by $0.85\% \text{ yr}^{-1}$ since 1986 (figure 2), accelerating from $0.29\% \text{ yr}^{-1}$ (1986–2000) to $1.59\% \text{ yr}^{-1}$ (2000–2016). Losses in the north were consistent between 1986 and 2016 ($1.02\% \text{ yr}^{-1}$), whereas initial increases between 1986 and 2000 ($1.95\% \text{ yr}^{-1}$) were replaced by losses between 2000 and 2016 ($2.11\% \text{ yr}^{-1}$) in southern Kenya. In the Watamu-Malindi region, a shallow reef system lost 77% of its seagrass in 30 years (figure 1), with rates of loss increasing from $0.73\% \text{ yr}^{-1}$ (1986–2000) to $4.64\% \text{ yr}^{-1}$ (2000–2016). Seagrass cover increased in Gazi ($0.95\% \text{ yr}^{-1}$) and Vanga ($0.34\% \text{ yr}^{-1}$) Bays between 1986 and 2000, then declined at $1.68\% \text{ yr}^{-1}$ and $1.8\% \text{ yr}^{-1}$, respectively. Pate Island suffered the largest total decline (figure 1), losing 40.09 km^2 ($1.5\% \text{ yr}^{-1}$) between 1986 and 2016.

S2-derived mapping accuracy from the field points was 73% (total), 76.7% (emergent) and 69.3% (submerged); we assume this is indicative for the whole region when estimating extent. Using the Landsat image overlap method, we estimated accuracies of 67.8%, 82.6% and 82.8% for the 1986, 2000 and 2016 maps, respectively. Emergent classification accuracy was also higher across all images (85.65%) compared to the submerged zones (80.03%).

Maximum total C loss from seagrass was 21.15% of the original over 30 years (table 1). Total C_{org} loss was estimated to be $0.07 \text{ Tg C yr}^{-1}$ using the regional estimate [3]; the

Table 1. Estimates of total C_{org} in Kenyan seagrass meadows.

year	regional carbon estimate (Tg c) ^a	global carbon estimate (Tg c) ^b
1986	10.28	7.16
2000	9.95	6.95
2016	8.11	5.78

^aBased on [3].

^bBased on [10].

global mean [10] gives an estimate of $0.05 \text{ Tg C yr}^{-1}$. The 2000–2016 acceleration in decline implied loss rates of $0.12 \text{ Tg C yr}^{-1}$ and $0.07 \text{ Tg C yr}^{-1}$ for the regional and global estimates, respectively. Total estimated C loss was 2.17 Tg over 30 years.

4. Discussion and conclusion

The last published estimate of seagrass coverage for Kenya is 112.39 km^2 [12], potentially underestimating the total area by 204.7 km^2 . Estimating total C from Kenyan seagrass using [10,12] gives 1.89 Tg , whereas our estimate of seagrass coverage and C_{org} from [3] gives 7.65 Tg C . If these figures are representative of Africa, global analyses of C storage in seagrass meadows are significantly underestimating the contribution from this region.

The rate of loss of seagrass in Kenya is below the global estimate of $7\% \text{ yr}^{-1}$ [1]. Patterns of loss vary between the north and south, with some regions (e.g. Malindi) showing more pronounced change. Slower rates of loss in Kenya may reflect historically low population sizes and industrialization. Kenyan population growth is approximately $2.9\% \text{ yr}^{-1}$ and is faster along the coast and in urban areas [13,14]; this driver probably underpins the accelerating rate of loss. Seagrass decline is often caused directly by fishing pressures and urban development and indirectly by eutrophication and climate change [15]. In sites such as Gazi Bay, we found numerous geometrical scars indicating fishing damage to seagrass meadows; anecdotal information suggests this occurs along the southern Kenya coast. Seagrass loss in the north may be related to the destruction of mangroves for large-scale irrigation, aquaculture and rice paddies [16,17] leading to sedimentation, thus reducing the area of seabed suitable for seagrasses. Because turbidity may prevent the detection of seagrass using remote sensing, our approach may not be as useful in areas with sporadically high turbidity if this occurs in the images used.

Promoting sustainable fishing practices, non-destructive land-use and communicating the importance of seagrass habitats should be at the forefront of management strategies. The role of seagrass as nurseries for fish has immediate traction for fishing communities, while including seagrass C in payments for ecosystem services schemes, such as that already operating for mangroves in Kenya [18] may bring new opportunities for conservation funds. African seagrass remains poorly researched; if these results are representative then global estimates of seagrass coverage and C stocks are underestimates.

Data accessibility. Supporting datasets have been uploaded to the Dryad repository: <https://doi.org/10.5061/dryad.n08qs2s> [9].

Authors' contributions. W.D.H., R.B. and M.H. conceived the initial project. W.D.H. analysed the satellite imagery and produced the results with the help of R.B. and M.H. M.H. helped conduct the field survey. All authors wrote the final manuscript. All authors agree to be held accountable for the content therein and approve the final version of the manuscript.

Competing interests. We declare we have no competing interests.

Funding. This work was funded by a grant from the British Council Newton Fund, grant no. 275670159.

Acknowledgements. We thank Ankje Frouws, Caroline Wanjiru, Peter Musembi, Tom Peter Kisiengo and Laitani Suleimani for their help in collecting groundtruthing data, staff at KMFRI Gazi for organization and the people of Gazi for hosting.

References

- Waycott M *et al.* 2009 Accelerating loss of seagrasses across the globe threatens coastal ecosystems. *Proc. Natl Acad. Sci. USA* **106**, 12 377–12 381. (doi:10.1073/pnas.0905620106)
- Githaiga MN, Gilpin L, Kairo JG, Huxham M. 2016 Biomass and productivity of seagrasses in Africa. *Bot. Mar.* **59**, 75. (doi:10.1515/bot-2015-0075)
- Githaiga MN, Kairo JG, Gilpin L, Huxham M. 2017 Carbon storage in the seagrass meadows of Gazi Bay, Kenya. *PLoS ONE* **12**, e0177001. (doi:10.1371/journal.pone.0177001)
- Hedley JD, Harborne AR, Mumby PJ. 2005 Simple and robust removal of sun glint for mapping shallow-water benthos. *Int. J. Remote Sens.* **26**, 2107–2112. (doi:10.1080/01431160500034086)
- Hochberg EJ, Atkinson MJ, Andréfouët S. 2003 Spectral reflectance of coral reef bottom-types worldwide and implications for coral reef remote sensing. *Remote Sens. Environ.* **85**, 159–173. (doi:10.1016/S0034-4257(02)00201-8)
- Stumpf RP, Holderied K, Sinclair M. 2003 Determination of water depth with high-resolution satellite imagery over variable bottom types. *Limnol. Oceanogr.* **48**, 547–556. (doi:10.4319/lo.2003.48.1_part_2.0547)
- McIntyre K, McLaren K, Prospere K. 2018 Mapping shallow nearshore benthic features in a Caribbean marine-protected area: assessing the efficacy of using different data types (hydroacoustic versus satellite images) and classification techniques. *Int. J. Remote Sens.* **39**, 1117–1150. (doi:10.1080/01431161.2017.1395924)
- Phinn SR, Roelfsema CM, Mumby PJ. 2012 Multi-scale, object-based image analysis for mapping geomorphic and ecological zones on coral reefs. *Int. J. Remote Sens.* **33**, 3768–3797. (doi:10.1080/01431161.2011.633122)
- Harcourt WD, Briers RA, Huxham M. 2018 Data from: The thin(ning) green line? Investigating changes in Kenya's seagrass coverage. Dryad Digital Repository. (doi:10.5061/dryad.n08qs2s)
- Fourqurean JW *et al.* 2012 Seagrass ecosystems as a globally significant carbon stock. *Nat. Geosci.* **5**, 505–509. (doi:10.1038/ngeo1477)
- Githaiga MN. 2016 *The role of seagrass meadows in Gazi Bay, Kenya as carbon sinks*. Edinburgh, UK: Napier.
- Short, T F. 2005 *Global distribution of seagrasses*. In *UNEP World Conserv. Monit. Cent. - Mar. metadata Cat*, pp. 13–15.
- Kenya. 2014 Demographic and Health Survey. See <https://dhsprogram.com/pubs/pdf/fr308/fr308.pdf>.
- Linard C, Kabaria CW, Gilbert M, Tatem AJ, Gaughan AE, Stevens FR, Sorichetta A, Noor AM, Snow RW. 2017 Modelling changing population distributions: an example of the Kenyan Coast, 1979–2009. *Int. J. Digit. Earth* **10**, 1017–1029. (doi:10.1080/17538947.2016.1275829)
- Orth RJ *et al.* 2006 A global crisis for seagrass ecosystems. *Bioscience* **56**, 987–996. (doi:10.1641/0006-3568(2006)56[987:agcfse]2.0.co;2)
- Kirui KB, Kairo JG, Bosire J, Viergever KM, Rudra S, Huxham M, Briers RA. 2013 Mapping of mangrove forest land cover change along the Kenya coastline using Landsat imagery. *Ocean Coast. Manag.* **83**, 19–24. (doi:10.1016/j.ocecoaman.2011.12.004)
- Abuodha PAW, Kairo JG. 2001 Human-induced stresses on mangrove swamps along the Kenyan coast. *Hydrobiologia* **458**, 255–265.
- Huxham M, Emerton L, Kairo J, Munyi F, Abdirizak H, Muriuki T, Nunan F, Briers RA. 2015 Applying climate compatible development and economic valuation to coastal management: a case study of Kenya's mangrove forests. *J. Environ. Manage.* **157**, 168–181. (doi:10.1016/j.jenvman.2015.04.018)